



# Accretion Flows in Binary stars with compact object

R. K. Zamanov

Institute of Astronomy and NAO, Bulgarian Academy of Sciences  
..... **KP-06-H98/8 "Accretion Flows in Binary stars"** .....

lecture notes in 01.04.02 "Astrophysics and Stellar astronomy"

These lecture notes are prepared as an aid to students and researchers involved in  
the project "Accretion Flows in Binary stars"

February 2026

# Contents

|          |  |           |
|----------|--|-----------|
| <b>1</b> | <b>Binary stars</b>                                  | <b>3</b>  |
| 1.1      | Constants . . . . .                                  | 3         |
| 1.2      | Kepler's third law . . . . .                         | 3         |
| 1.3      | Roche lobe size . . . . .                            | 4         |
| <b>2</b> | <b>White Dwarfs</b>                                  | <b>5</b>  |
| 2.1      | White Dwarfs and Nova eruption . . . . .             | 6         |
| 2.2      | White Dwarfs and type Ia supernova . . . . .         | 6         |
| <b>3</b> | <b>Gravimagnetic rotators</b>                        | <b>7</b>  |
| <b>4</b> | <b>Accretion discs</b>                               | <b>10</b> |
| 4.1      | Radial distribution of temperature in disc . . . . . | 10        |
| 4.2      | Boundary layer . . . . .                             | 13        |
| <b>5</b> | <b>Novae and Recurrent Novae</b>                     | <b>16</b> |
| 5.1      | Acretion and Nova eruption . . . . .                 | 16        |
| <b>6</b> | <b>Rozhen Echelle-ESpeRo spectra</b>                 | <b>18</b> |

# Chapter 1

## Binary stars

### 1.1 Constants

Here are given the numerical values of a few constants in cgs-system often used in astrophysics of binary stars:

Gravitational constant  $G = 6.67 \cdot 10^{-8} \text{ cm}^3 \text{ g}^{-1} \text{ s}^{-2}$

Stefan-Boltzman  $\sigma = 5.67 \cdot 10^{-5} \text{ erg cm}^{-2} \text{ s}^{-1} \text{ K}^{-4}$

Mass of the Sun  $M_{\odot} = 1.99 \cdot 10^{33} \text{ g}$

Radius of the Sun  $R_{\odot} = 6.96 \cdot 10^{10} \text{ cm}$

Solar Luminosity  $L_{\odot} = 3.85 \cdot 10^{33} \text{ erg s}^{-1}$

### 1.2 Kepler's third law

In binary stars the two stars with masses  $M_1$  and  $M_2$  orbit each other in a orbit with semimajor axis  $a$ . The orbital frequency  $\Omega$ , and the orbital period  $P_{orb}$  are connected with the masses (Kepler's third law) as

$$\Omega = \frac{2\pi}{P_{orb}} \quad (1.1)$$

$$\Omega^2 = G(M_1 + M_2)/a^3 \quad (1.2)$$

$$P_{orb}^2 = \frac{4\pi^2 a^3}{G(M_1 + M_2)} \quad (1.3)$$

The binary stars lose angular momentum through gravitational radiation and wind from the secondary. Due to these losses the separation between the stars decreases and the size of the Roche lobes decrease.

The distance between the components at periastron and apastron is

$$a_{per} = a(1 - e) \quad (1.4)$$

$$a_{ap} = a(1 + e) \quad (1.5)$$

### 1.3 Roche lobe size

For calculation of the Roche lobe size in binary stars, one of the most used is the formula (Eggleton, P. P., 1983, "Approximations to the radii of Roche lobes". The Astrophysical Journal, vol. 268, p. 368):

$$\frac{R_L}{a} = \frac{0.49 q^{2/3}}{0.6q^{2/3} + \ln(1 + q^{1/3})} \quad (1.6)$$

where  $q = M_1/M_2$

Figures presenting the Lagrangian points can be seen on:

[https://en.wikipedia.org/wiki/Lagrange\\_point](https://en.wikipedia.org/wiki/Lagrange_point)

<http://hyperphysics.phy-astr.gsu.edu/hbase/Mechanics/lagpt.html>

Figures presenting the shape of the Roche lobe can be seen on:

[https://en.wikipedia.org/wiki/Roche\\_lobe](https://en.wikipedia.org/wiki/Roche_lobe)

<https://astronomy.swin.edu.au/cosmos/r/roche-lobe>

# Chapter 2

## White Dwarfs

The majority of all stars in the Milky Way will one day become white dwarfs. The white dwarfs are objects in which electron degeneracy pressure is equal to the gravitational pressure. Remarkable properties are that (1) the more massive white dwarfs are smaller. (2) the mass radius relation sets an upper limit to the mass of the white dwarfs above which the electron degeneracy can no longer support the gravitational force, and they explode as type Ia supernova. This limit is estimated  $1.44 M_{\odot}$  (Chandrasekhar 1931, *Astrophysical Journal*, 74, 81).

We note in passing that there are some indications that strong magnetic field can increase this upper limit. For example, Franzon & Schramm (2017, IOP Conf. Series: Journal of Physics: Conf. Series 861, 012015, doi:10.1088/1742-6596/861/1/012015, "Effects of magnetic fields in white dwarfs") obtained strongly magnetized white dwarfs with masses  $M \sim 2.0 M_{\odot}$ .

One can find different formulae for the connection between the mass and the radius of the white dwarfs. We will use here Eggleton's formula as given in Verbunt & Rappaport (1988, *Astrophysical Journal*, 332, 193):

$$\frac{R_{wd}}{R_{\odot}} = 0.0114 \left[ \left( \frac{M_{wd}}{M_{Ch}} \right)^{-2/3} - \left( \frac{M_{wd}}{M_{Ch}} \right)^{2/3} \right]^{1/2} \left[ 1 + 3.5 \left( \frac{M_{wd}}{M_p} \right)^{-2/3} + \left( \frac{M_{wd}}{M_p} \right)^{-1} \right]^{-2/3} \quad (2.1)$$

where  $M_{Ch}$  is the Chandrasekhar limit mass for the white dwarfs  $M_{Ch} = 1.44 M_{\odot}$ ,  $M_p$  is a constant  $M_p = 0.00057 M_{\odot}$ . The white dwarfs masses are in the range  $0.2-1.4 M_{\odot}$ , and their radii are in the range  $0.005-0.02 R_{\odot}$  (4000 - 16000 km).

A typical white dwarf with  $0.9 M_{\odot}$  has a radius 6500 km, which is similar to the size of the Earth. The density is  $1500 \text{ kg/cm}^3$  (!). An other interesting point is that the more massive white dwarfs are smaller, for example a  $0.40 M_{\odot}$  white dwarf has a radius 10675 km, a three times more massive  $1.2 M_{\odot}$  white dwarf has 2.8 times smaller radius 3859 km.

There are a few tests of this relation. As an example in Fig. 2.1, are plotted a few white dwarfs with estimated masses and radii. They are taken from Parsons et al.

(2017, MNRAS, 470, 4473), where masses and radii are estimated for white dwarfs in detached eclipsing binaries. Double-lined eclipsing binaries are good sources for mass-radius measurements. The observed white dwarfs indicate that the theoretical relation gives good result.

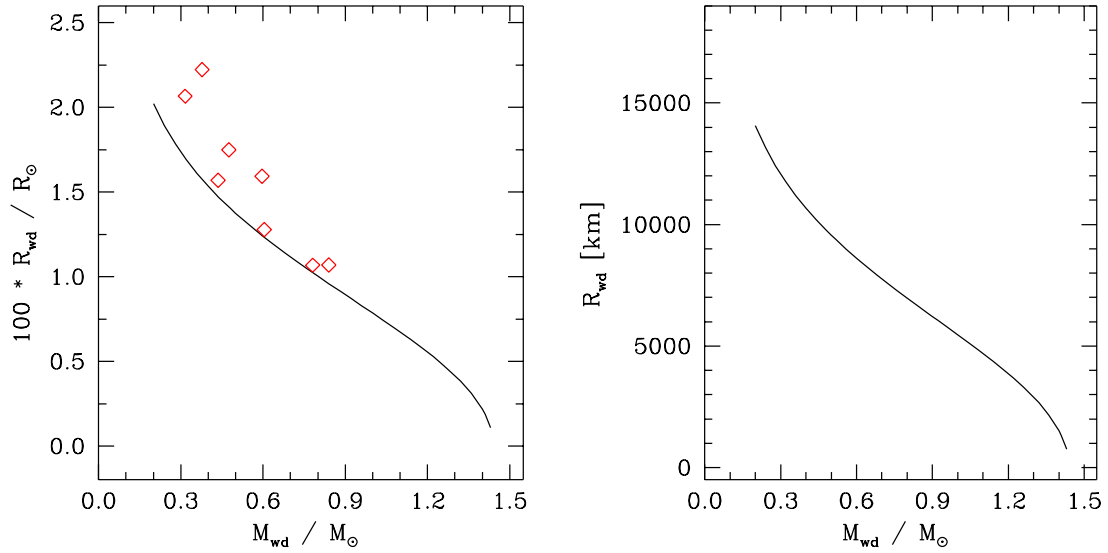


**Figure 2.1:** Mass-radius relation for white dwarfs. The left panel represents the radius of the white dwarf in solar radii. Eight white dwarfs, with known masses are also plotted. In the right panel is the same relation with Y-axis in km.

## 2.1 White Dwarfs and Nova eruption

When hydrogen rich material accretes on the white dwarf surface it will form an envelope around it. When the pressure at the base of the envelope exceeds the critical value an ignition of thermo-nuclear runaway occurs. The white dwarf undergoes Nova eruption.

## 2.2 White Dwarfs and type Ia supernova

type Ia Supernova, when the mass of the white dwarf exceeds the Chandrasekhar limit at  $M_{\text{wd}} = 1.44 M_{\odot}$ , the core of the white dwarf reaches ignition for carbon fusion, energy  $10^{51}$  erg, absolute V band magnitude  $M_V = -19.3$ .

# Chapter 3

## Gravimagnetic rotators

Unusual signals from pulsating radio sources have been recorded at the Mullard Radio Astronomy Observatory. The radiation seems to come from local objects within the galaxy, and may be associated with oscillations of white dwarf or neutron stars.

Most, if not all, neutron stars descend from main sequence stars with  $m_a$ , i.e., O and early B stars, while lower mass main sequence stars give rise to white dwarfs.

The majority of the neutron stars are late stages of the evolution of stars, which during their life on the main-sequence had masses  $M_{MS} > 8 \text{ M}_\odot$ . These are O and early B stars. Stars which on the main sequence have lower masses (less than  $8 \text{ M}_\odot$ ) give rise to white dwarfs.

The neutron stars have strong magnetic fields, in the range  $10^8 - 10^{15}$  Gauss. The majority of the radio pulsars have magnetic fields, in the range  $10^{11} - 10^{13}$  G. The magnetic white dwarfs in the polars have strength of the magnetic field is  $10^6 - 10^8$  G.

A rotating compact object (neutron star or white dwarf) has both strong gravitational and strong magnetic field. The interaction of such an object with the surrounding matter can be in different regimes: accretor, propeller, ejector, georotator, magnetar. The type of the regime depends on its rotational period, strength of its magnetic field, the density and the velocity of the surrounding material. Hereafter we will speak about the neutron stars, however the same equations (with some very small modifications are also valid for white dwarfs.)

Here we give a few characteristic parameters. Their ratios determine in which regime will the neutron star be.

1. **Accretion radius**,  $R_a$  (often also named gravitational capture radius), is the distance at which the kinetic energy of the matter is equal to its potential energy in the gravitational field of the compact object:

$$\frac{V_{rel}^2}{2} = \frac{GM}{R_a}, \quad (3.1)$$

$$R_a = \frac{2GM_{ns}}{V_{rel}^2} \quad (3.2)$$

where  $G$  is the gravitational constant,  $M$  is the mass of the neutron star,  $V_{rel}$  is the relative velocity between the neutron star and wind of the mass donor. If the matter is closer to the neutron star than  $R_a$ , it will be captured in the gravitational field of the neutron star. A more accurate formula for  $R_a$  includes also the speed of sound  $c_s$  in the surrounding matter:

$$R_a = \frac{2GM}{V_{rel}^2 + c_s^2}. \quad (3.3)$$

In binary stars usually  $V_{rel} > c_s$ , and Eq. 3.2 is a good approximation.

**2. Radius of the light cylinder**,  $R_l$ , is the distance at which, the rotational speed of the magnetic field is equal to the speed of light ( $c = 3.10^{10}$  cm s $^{-1}$ ). At distances closer than  $R_l$ , the magnetic field of the neutron star is a rotating dipole, at distances larger than  $R_l$  it is free propagating electromagnetic wave

### 3. Radius of the magnetosphere (Alfvén radius)

$$R_m = \left( \frac{\mu^2}{\dot{M}_c \sqrt{2GM_{ns}}} \right)^{\frac{2}{7}}, \quad (3.4)$$

**4. Accretion luminosity** - when material is accreting onto the neutron star surface, it will generate luminosity:

$$L_a = \frac{GM_{ns}\dot{M}_c}{R_{ns}}, \quad (3.5)$$

where  $\dot{M}_c$  is the mass capture rate,  $M_{ns}$  is the mass of the neutron star,  $R_{ns}$  is the radius of the neutron star. Example: at mass capture rate  $10^{-9} M_{\odot}$  yr $^{-1}$ , a neutron star will generate accretion luminosity .... . At the same mass accretion rate an  $1 M_{\odot}$  white dwarf will generate accretion luminosity ....

When a neutron star is in regime propeller (also named accretion onto the magnetosphere), the accreting material does not achieve its surface. It is stopped at the boundary of the magnetosphere, and after it is ejected outward as blobs. The luminosity is:

$$L_a = \frac{GM_{ns}\dot{M}_c}{R_m}. \quad (3.6)$$

In this regime neutron star spins-down very effectively. Because  $R_m \gg R_{ns}$ , the X-ray luminosity generated from a propeller is considerably lower than from an accretor.

For example for the observation of the transient X-ray pulsar 4U 0115+63 (Campana et al., 2001, The Astrophysical Journal, vol. 561, pp. 924-929), led to the discovery of a dramatic luminosity variation from  $2.10^{34}$  to  $5.10^{36}$  ergs s $^{-1}$  (which is a factor of  $\approx 250$ ), as a result of the transition from propeller to accretor regime.

We note, that when the mass-accretion rate exceeds the Eddington rate, a significant fraction of the accreting gas is expelled as a superwind or jets (these type of regimes are named super-accretor, super-propeller, and super-ejector). The Eddington luminosity was introduced in the context of luminous stars: for any star, there is a maximum luminosity beyond which radiation pressure will overcome gravity, and material outside the object will be forced away from it (stellar wind) rather than falling inwards (accretion).

# Chapter 4

## Accretion discs

The accretion discs are formed when material from the surrounding environment is captured by an object with strong gravitational field.

The accretion discs are observed in variety of objects, among them: (1) around white dwarfs in Cataclysmic variable stars, (2) around white dwarfs in symbiotic stars, (3) around neutron stars in High Mass and Low mass X-ray binaries, (4) in T Tauri stars, (5) around black holes in X-ray binaries. They also probably exist around supermassive black holes in Active Galactic Nuclei. There are thousands of scientific papers discussing different properties of the accretion discs, and we can say that a new scientific field exists during the last years – discology.

### 4.1 Radial distribution of temperature in disc

In Cataclysmic variables the secondary is a red dwarf, in the most cases in the spectral range K0V-M6V. It fulfills its Roche lobe, and as a result the gas from its outer parts overflow through the inner Lagrangian point and forms a stream to the white dwarf. The gas moves in a spiral pattern to the white dwarf surface. During the process part of the gravitational energy is emitted. For a disc to be in steady state is necessary that the emitted energy is equal to the released gravitational energy. If the disc is optically thick in the  $z$  direction (the vertical direction), it radiates as a black body with effective temperature given by the standard relation  $\sigma T^4$ . For a ring with size  $dR$  located at distance  $R$  from the white dwarf the emitted energy is:

$$\Delta E = \sigma T^4 2\pi R dR, \quad (4.1)$$

where  $\sigma = 5.67 \cdot 10^{-5}$  erg cm $^{-2}$  s $^{-1}$  K $^{-4}$  is the Stefan Boltzmann constant,  $R$  is the distance from the white dwarf. (The potential energy per unit mass at radius  $R$  is  $E = -GM/R$ .) The difference of the gravitational energy (potential energy) between the outer and inner edge of the ring is:

$$\Delta E = \frac{GM_{wd} \dot{M}_a}{R} - \frac{GM_{wd} \dot{M}_a}{R + dR} \quad (4.2)$$

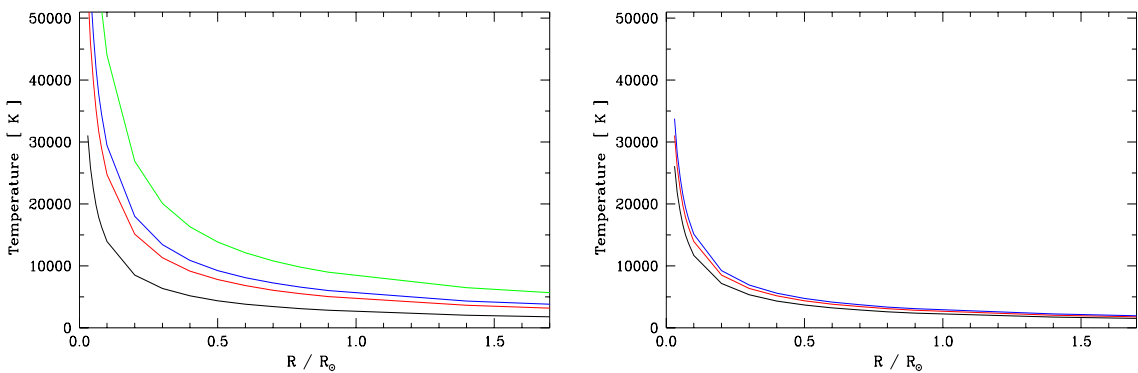


**Figure 4.1:** Temperature in accretion disc around white dwarf. The X-axis is the distance from the white dwarf. The Y-axis is the local temperature in the disc.

The left panel represents the dependance on the mass accretion rate. The lines are for  $M=1 M_{\odot}$  white dwarf and mass accretion rates  $10^{-9}$  (black),  $10^{-8}$  (red),  $2.10^{-8}$  (blue),  $10^{-7}$  (green)  $M_{\odot} \text{ yr}^{-1}$ .

The right panel represents the dependance on the white dwarf mass. The lines are for mass accretion rate  $10^{-9} M_{\odot} \text{ yr}^{-1}$ , and white dwarf masses  $0.5 M_{\odot}$  (black),  $1 M_{\odot}$  (red),  $1.4 M_{\odot}$  (blue).

We obtain

$$T^4 = \frac{GM_{wd} \dot{M}_a}{2\pi\sigma R dR} \left( \frac{1}{R} - \frac{1}{R + dR} \right) \quad (4.3)$$

$$T^4 = \frac{GM_{wd} \dot{M}_a}{2\pi\sigma R} \left( \frac{1}{R^2 + R dR} \right) \quad (4.4)$$

Having in mind that  $dR \ll R$ , we obtain

$$T^4 = \frac{G M_{wd} \dot{M}_a}{2\pi \sigma R^3} \quad (4.5)$$

More detailed calculations account for (1) radial energy flux through the disc (transport of angular momentum also means transport of energy) and (2) boundary conditions at the inner edge of the disc and give:

$$T_{eff}^4 = \frac{3 G \dot{M}_a M_{wd}}{8\pi \sigma R^3} \left[ 1 - \left( \frac{R_{wd}}{R} \right)^{1/2} \right] \quad (4.6)$$

In Fig. 4.1 are plotted colour lines for different white dwarf masses and mass accretion rates.

In the case of accretion disc around a neutron star  $R_{wd}$  must be replaced with the radius of the neutron star. In case of accretion disc around a black hole (stellar mass black hole or supermassive black hole) it must be replaced with the Schwarzschild radius  $R_s = 2GM/c^2$ .

## 4.2 Boundary layer

In an accretion disc the particles rotate around the white dwarf at Keplerian velocities. At the last orbit above the white dwarf surface the gas has kinetic energy per unit mass  $E_k = V^2/2$ , where  $V$  is the Keplerian velocity  $V = (GM_{wd}/R)^{1/2}$ . The total energy emitted in the accretion disc is the difference between the potential energy and the kinetic energy:

$$L_{disc} = \frac{GM_{wd}\dot{M}_a}{R_{wd}} - \frac{\dot{M}_a V^2}{2}. \quad (4.7)$$

Replacing the velocity  $V$  with the Keplerian velocity, we obtain

$$L_{disc} = \frac{GM_{wd}\dot{M}_a}{2 R_{wd}}. \quad (4.8)$$

The accretion disc emits about half (50%) of the total accretion energy. If the white dwarf is non-rotating (or slow rotating) the other half of the accretion energy will be emitted by the boundary layer between the white dwarf and the accretion disc. Because the size of the boundary layer is small it will be very hot.

$$4\pi R_{wd}^2 \sigma T_{bl}^4 = \frac{G M_{wd} \dot{M}_a}{2 R_{wd}} \quad (4.9)$$

The temperature of a thin boundary layer between  $1.0 M_{\odot}$  white dwarf accreting at  $10^{-9} M_{\odot} \text{ yr}^{-1}$  is expected to be of about  $10^5 \text{ K}$ . Because in the real cases the boundary layer is not thin, it will probably have a size  $2 - 5 R_{wd}$ , and temperarure  $60000 \text{ K} - 30000 \text{ K}$ . In the Fig. 4.2 is plotted  $T_{bl}$  versus  $\dot{M}_a$  and versus the size of the boundary layer. In the left panel is visible that when the  $\dot{M}_a$  increases the  $T_{bl}$  also increases. In the right panel is visible that when the size of the boundary layer increases  $T_{bl}$  decreases. It is also visible that more massive white dwarfs are expected to have hotter boundary layer.

A thermal spectrum of a black body with temperature  $T$  peaks at frequency

$$h\nu = 2.8 k T \quad (4.10)$$

or

$$\frac{h c}{\lambda} = 2.8 k T \quad (4.11)$$

$$\lambda = \frac{h c}{2.8 k T} \quad (4.12)$$

where the Planck constant is  $h = 6.63 \times 10^{-27} \text{ erg s}$  and Boltzman constant is  $k = 1.38 \times 10^{-16} \text{ erg/K}$ . A boundary layer with  $T_{BL} = 50000 \text{ K}$  will emit maximum radiation at  $1030 \text{ \AA}$ , with  $T_{BL} = 10^5 \text{ K}$  the maximum of the radiation will be at  $515 \text{ \AA}$ .

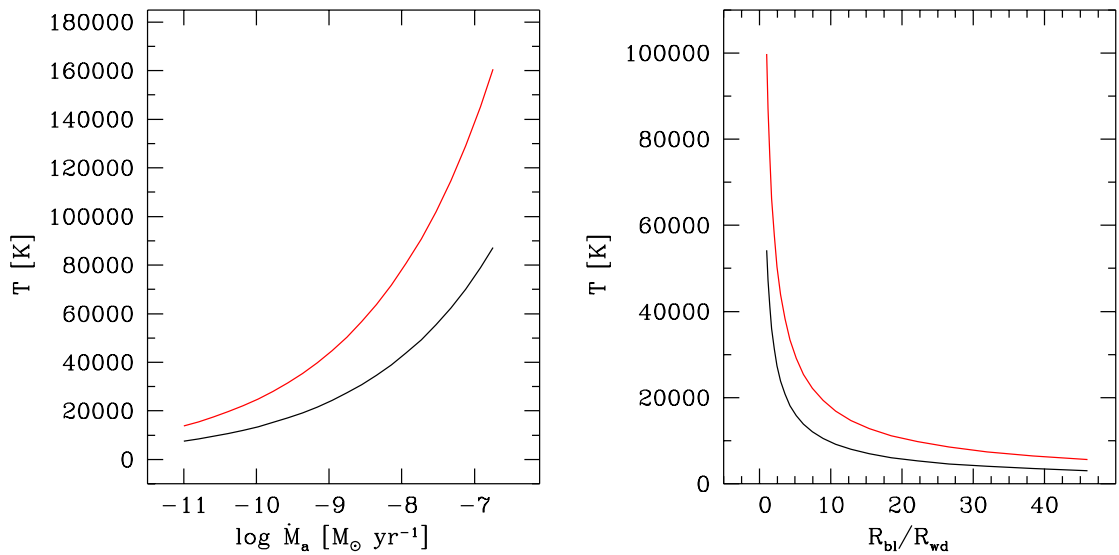


**Figure 4.2:** Temperature of the boundary layer. The left panel is the temperature of the boundary layer versus mass accretion rate, adopting size of the boundary layer  $3 R_{wd}$ . The lines are for mass of the white dwarf  $0.5 M_{\odot}$  (black) and  $1 M_{\odot}$  (red). The right panel represents the temperature versus the size of the boundary layer. The lines are for mass accretion rate  $10^{-9} M_{\odot} \text{ yr}^{-1}$ , and white dwarf masses  $0.5 M_{\odot}$  (black) and  $1 M_{\odot}$  (red).

The ultraviolet radiation (UV), defined most broadly as 100-4000 Å, can be subdivided into a number of ranges recommended by the ISO standard ISO 21348. near UV (3000-4000 Å), middle UV (2000-3000 Å), far UV (1220 - 2000 Å), extreeme UV (100 - 1220 Å). A boundary layer around an white dwarf is expected to emit in the far UV.

# Chapter 5

## Novae and Recurrent Novae

According to the thermonuclear runaway model, novae and recurrent novae are powered by thermonuclear explosions in the hydrogen-rich envelopes formed around the surface of white dwarfs. The novae eruptions play a role in the enrichment of the interstellar medium through a number of intermediate-mass elements. This includes  $^{17}O$ ,  $^{15}N$ , and  $^{13}C$ , systematically overproduced with respect to solar abundances, plus a lower contribution in a number of other species ( $A < 40$ ), such as  $^7Li$ ,  $^{19}F$ , or  $^{26}Al$ . When a white dwarf is a member of a binary system it will accrete material from its companion. In Cataclysmic variable stars its companion is a red dwarf of spectral type K1V - M4V. In the Symbiotic stars the white dwarfs accrete material from red giant of spectral type K1III - M8III.

### 5.1 Accretion and Nova eruption

When hydrogen rich material accretes on the white dwarf surface it will form an envelope around it. The mass of the envelope increases during the accretion process:

$$M_{env} = \dot{M}_{acc} \Delta t, \quad (5.1)$$

where  $M_{env}$  is the mass of the envelope,  $\dot{M}_{acc}$  is the mass accretion rate,  $\Delta t$  is the elapsed time.

The pressure at the base of the envelope is:

$$P_{base} = \frac{G M_{wd} M_{env}}{4\pi R_{wd}^4}, \quad (5.2)$$

where  $G$  is the gravitational constant  $G = 6.67 \times 10^{-8} \text{ cm}^3 \text{ g}^{-1} \text{ s}^{-2}$ ,  $M_{wd}$  and  $R_{wd}$  are the white dwarf mass and radius, respectively. In this equation  $4\pi R_{wd}^2$  represents the area of the white dwarf's surface,  $G M_{wd} M_{env} / R_{wd}^2$  is the weight of the envelope (the gravitational force) in the white dwarf gravitational field.

The pressure at the base of the envelope increases with time:

$$P_{base} = \frac{G M_{wd} \dot{M}_{acc} \Delta t}{4\pi R_{wd}^4}, \quad (5.3)$$

and when the pressure exceeds the critical value an igniton of thermo-nuclear runaway occurs. The critical value is estimated to be  $P_{crit} \approx 2 \times 10^{19}$  dyne cm<sup>-2</sup> (Livio 1983, *Astronomy and Astrophysics*, 12, L7).

As examples, of the application of the above formulae, we estimate the time necessary for the envelope to achieve the critical pressure (and ignite TNR):

$$M_{wd} = 0.5 M_{\odot}, \dot{M}_{acc} = 1.10^{-9} M_{\odot} \text{ yr}^{-1}, \Delta t = 2.10^6 \text{ yr} ;$$

$$M_{wd} = 1.0 M_{\odot}, \dot{M}_{acc} = 1.10^{-9} M_{\odot} \text{ yr}^{-1}, \Delta t = 1.10^5 \text{ yr} ;$$

$$M_{wd} = 1.4 M_{\odot}, \dot{M}_{acc} = 1.10^{-9} M_{\odot} \text{ yr}^{-1}, \Delta t = 416 \text{ yr}$$

The recurrent nova RS Oph has recorded outbursts in 1985, 2006, and 2021. The recurrence time is about 20 years. From the above formulae we expect that the white dwarfs is massive,  $M_{wd} = 1.4 M_{\odot}$  (close to the Chandrasekar limit), its radius is small  $R_{wd} = 1600$  km, mass accretion rate is high,  $2.10^{-8} M_{\odot} \text{ yr}^{-1}$ . With this set of parameters, we calculate a recurrence time 21 yr. In other words to have a nova outburst every 20 years, the white dwarf should be massive and to accrete at high accretion rate.

Questions to think about:

what is the thickness of the envelope?

what is the influence of the stellar spin on the ignition of the thermonuclear runaway?

# Chapter 6

## Rozhen Echelle-ESpeRo spectra

Here is given a simple way to reduce Rozhen Echelle-ESpeRo spectra using IRAF.

1. Preparation (start IRAF):

```
cl > noao  
cl > imred  
cl > echelle
```

```
cl > files *.fits > li.1  
cl > copy ThAr1.30s.fits th1.fits
```

```
cl > hedit @li.1 dispaxis 1 add+  
cl > hedit @li.1 imagetyp object add+
```

```
cl > copy HD138749.600s.fits a1.fits  
... a1.fits - must be a bright star
```

2. we start *apall* over the spectrum of the bright star *a1.fits*. Here are given the parameters of *apall*.

```

cl > epar apall
I R A F
Image Reduction and Analysis Facility
PACKAGE = echelle
TASK = apall

input = a1.fits List of input images
(output = ) List of output spectra
(apertur= ) Apertures
(format = multispec) Extracted spectra format
(referen= a1.fits) List of aperture reference images
(profile= ) List of aperture profile images

(interac= yes) Run task interactively?
(find = yes) Find apertures?
(recente= yes) Recenter apertures?
(resize = yes) Resize apertures?
(edit = yes) Edit apertures?
(trace = yes) Trace apertures?
(fittrac= yes) Fit the traced points interactively?
(extract= yes) Extract spectra?
(extras = no) Extract sky, sigma, etc.?
(review = no) Review extractions?

(line = 970) Dispersion line
(nsum = 20) Number of dispersion lines to sum or median

# DEFAULT APERTURE PARAMETERS
(lower = -5.) Lower aperture limit relative to center
(upper = 5.) Upper aperture limit relative to center
(apidtab= ) Aperture ID table (optional)

# DEFAULT BACKGROUND PARAMETERS
(b_funct= chebyshev) Background function
(b_order= 2) Background function order
(b_sampl= -17:-5,5:17) Background sample regions
(b_naver= 0) Background average or median
(b_niter= 5) Background rejection iterations
(b_low_r= 4.) Background lower rejection sigma
(b_high_r= 2.) Background upper rejection sigma
(b_grow = 0.) Background rejection growing radius

```

```

# APERTURE CENTERING PARAMETERS
(width =      5.)  Profile centering width
(radius =    10.)  Profile centering radius
(thresho=    0.)  Detection threshold for profile centering

# AUTOMATIC FINDING AND ORDERING PARAMETERS
nfind =          60  Number of apertures to be found automatically
(minsep =      12.) Minimum separation between spectra
(maxsep =      55.) Maximum separation between spectra
(order =  increasing) Order of apertures

# RECENTERING PARAMETERS
(aprecen=      ) Apertures for recentering calculation
(npeaks =  INDEF) Select brightest peaks
(shift =      yes) Use average shift instead of recentering?

# RESIZING PARAMETERS
(llimit =  INDEF) Lower aperture limit relative to center
(ulimit =  INDEF) Upper aperture limit relative to center
(ylevel =      0.1) Fraction of peak or intensity for automatic width
(peak =      yes) Is ylevel a fraction of the peak?
(bkg =      yes) Subtract background in automatic width?
(r_grow =      1.) Grow limits by this factor
(avglimi =     no) Average limits over all apertures?

# TRACING PARAMETERS
(t_nsum =      10) Number of dispersion lines to sum
(t_step =      10) Tracing step
(t_nlost=      3) Number of consecutive times profile is lost before quitting
(t_funct=  legendre) Trace fitting function
(t_order=      5) Trace fitting function order
(t_sampl=      *) Trace sample regions
(t_naver=      1) Trace average or median
(t_niter=      0) Trace rejection iterations
(t_low_r=      3.) Trace lower rejection sigma
(t_high_r=      3.) Trace upper rejection sigma
(t_grow =      0.) Trace rejection growing radius

```

```
# EXTRACTION PARAMETERS
(backgro=      fit)  Background to subtract
(skybox =      1)    Box car smoothing length for sky
(weights=      none) Extraction weights (none—variance)
(pfit =       fit1d) Profile fitting type (fit1d—fit2d)
(clean =      no)   Detect and replace bad pixels?
(saturat=    INDEF) Saturation level
(readnoi=      1)    Read out noise sigma (photons)
(gain =       1.)   Photon gain (photons/data number)
(lsigma =      4.)   Lower rejection threshold
(usigma =      4.)   Upper rejection threshold
(nsubaps=     1)    Number of subapertures per aperture
(mode =       ql)
```

3. start "apall" on @li.1 using a1.fits as a reference image.

*cl > epar apall*

I R A F

Image Reduction and Analysis Facility

PACKAGE = echelle

TASK = apall

|           |            |                                      |
|-----------|------------|--------------------------------------|
| input =   | @li.1      | List of input images                 |
| (output = | )          | List of output spectra               |
| (apertur= | )          | Apertures                            |
| (format = | multispec) | Extracted spectra format             |
| (referen= | a1.fits)   | List of aperture reference images    |
| (profile= | )          | List of aperture profile images      |
| (interac= | yes)       | Run task interactively?              |
| (find =   | no)        | Find apertures?                      |
| (recente= | no)        | Recenter apertures?                  |
| (resize = | no)        | Resize apertures?                    |
| (edit =   | no)        | Edit apertures?                      |
| (trace =  | no)        | Trace apertures?                     |
| (fittrac= | no)        | Fit the traced points interactively? |
| (extract= | yes)       | Extract spectra?                     |
| (extras = | no)        | Extract sky, sigma, etc.?            |
| (review = | no)        | Review extractions?                  |

... ... the other parameters are as above.

bf 4. Identifying of Th-Ar lines on *th1.ms.fits*.

*ec > epar* eidentify

I R A F  
 Image Reduction and Analysis Facility  
 PACKAGE = echelle  
 TASK = eidentify

|           |                      |   |
|-----------|----------------------|---|
| images =  | th1.ms.fits          | Images containing features to be identified             |
| (databas= | database)            | Database in which to record feature data                |
| (coordli= | linelists\$thar.dat) | User coordinate list                                    |
| (units =  | )                    | Coordinate units  |
| (match =  | 0.085)               | Coordinate list matching limit in user units            |
| (maxfeat= | 5550)                | Maximum number of features for automatic identification |
| (zwidth = | 10.)                 | Zoom graph width in user units                          |
| (ftype =  | emission)            | Feature type  |
| (fwidth = | 4.)                  | Feature width in pixels                                 |
| (cradius= | 5.)                  | Centering radius in pixels                              |
| (thresho= | 100.)                | Feature threshold for centering                         |
| (minsep = | 2.)                  | Minimum pixel separation                                |
| (functio= | chebyshev)           | Coordinate function                                     |
| (xorder = | 3)                   | Order of coordinate function along dispersion           |
| (yorder = | 3)                   | Order of coordinate function across dispersion          |
| (niterat= | 0)                   | Rejection iterations                                    |
| (lowreje= | 2.5)                 | Lower rejection sigma                                   |
| (highrej= | 2.5)                 | Upper rejection sigma                                   |
| (autowri= | no)                  | Automatically write to database?                        |
| (graphic= | stdgraph)            | Graphics output device                                  |
| (cursor = | )                    | Graphics cursor input                                   |
| (mode =   | ql)                  |   |

For the fitting we usually use the orders H-alpha, Ha-1, Ha+4, Ha+36 (see the figures)  
 Usually, we mark 5-6 lines on orders  $H\alpha$  ( $\lambda 6562$ ) and  $\lambda 6240$  and 3-4 lines on other orders.

**keys:** m - mark, f-fit, l-lines (finding of lines), q - quit

After the initial fit, *xorder* and *yorder* must be changed:  
 (*xorder* = 6) Order of coordinate function along dispersion  
 (*yorder* = 6) Order of coordinate function across dispersion

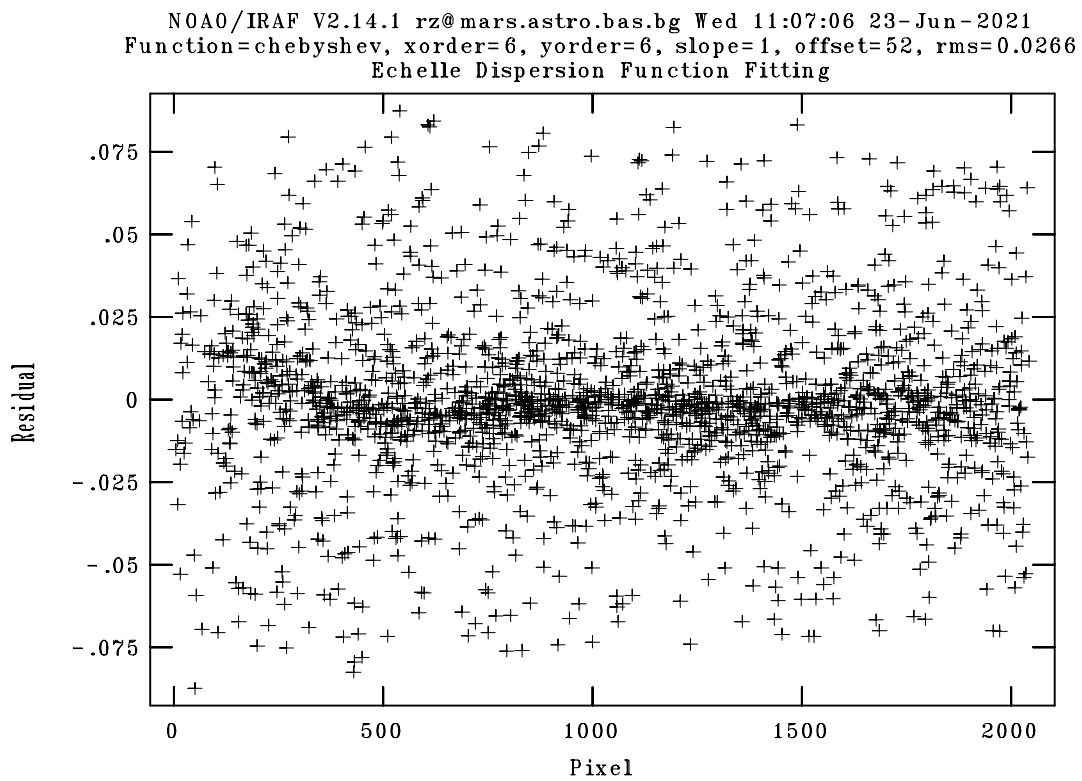


**Figure 6.1:** The final result of the fitting with *ecidentify*.

The final result of the fitting can be seen on Fig. 6.1.

Example of file *li.1*:

HD109358.180s.fits  
HD138749.600s.fits  
MWC656.2400s.fits  
SULyn.fits  
flat01.fits  
ThAr.10s.fits  
ThAr.30s.fits  
th1.fits

Example of file *li.2*

HD109358.180s.ms.fits  
HD138749.600s.ms.fits  
MWC656.2400s.ms.fits  
SULyn.ms.fits  
flat01.ms.fits  
ThAr.10s.ms.fits  
ThAr.30s.ms.fits

Example of file *li.3*

HD109358.180s.20210524.fit  
HD138749.600s.20210524.fit  
MWC656.2400s.20210524.fit  
SULyn.20210524.fit  
flat01.20210524.fit  
ThAr.10s.20210524.fit  
ThAr.30s.20210524.fit

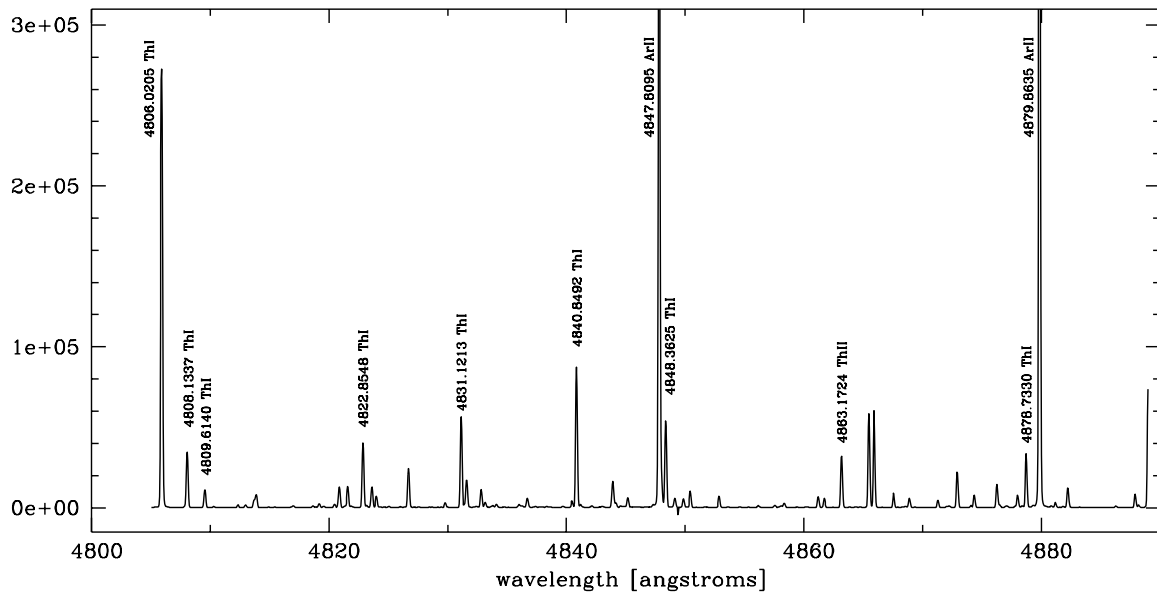


Figure 6.2: Th-Ar spectrum around  $\lambda 4860 \text{ \AA}$  ( $H\beta$  line).

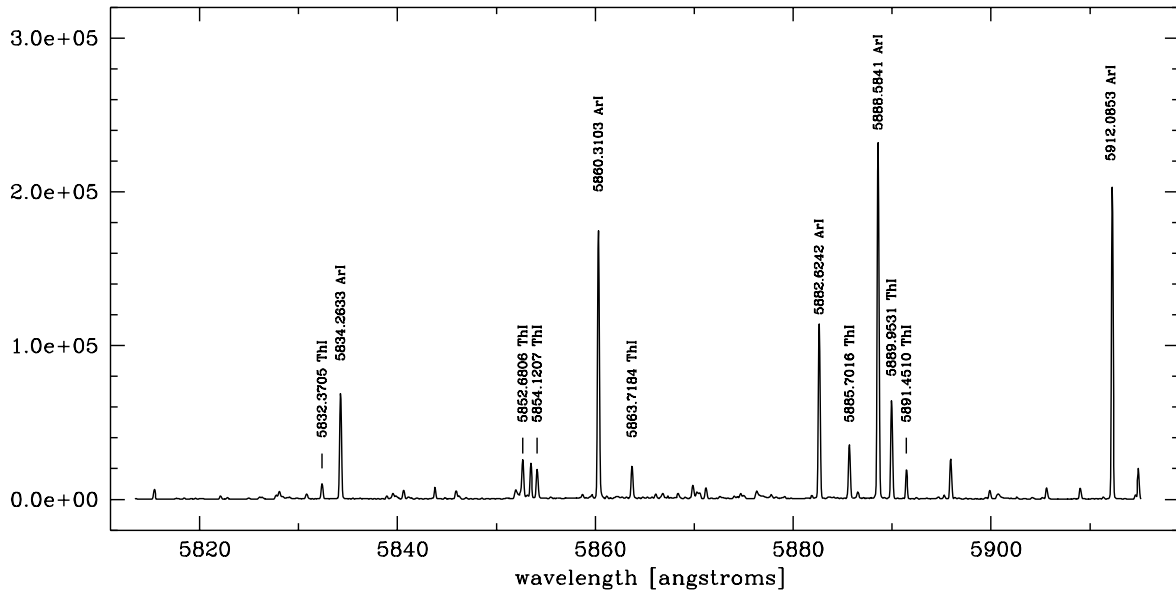
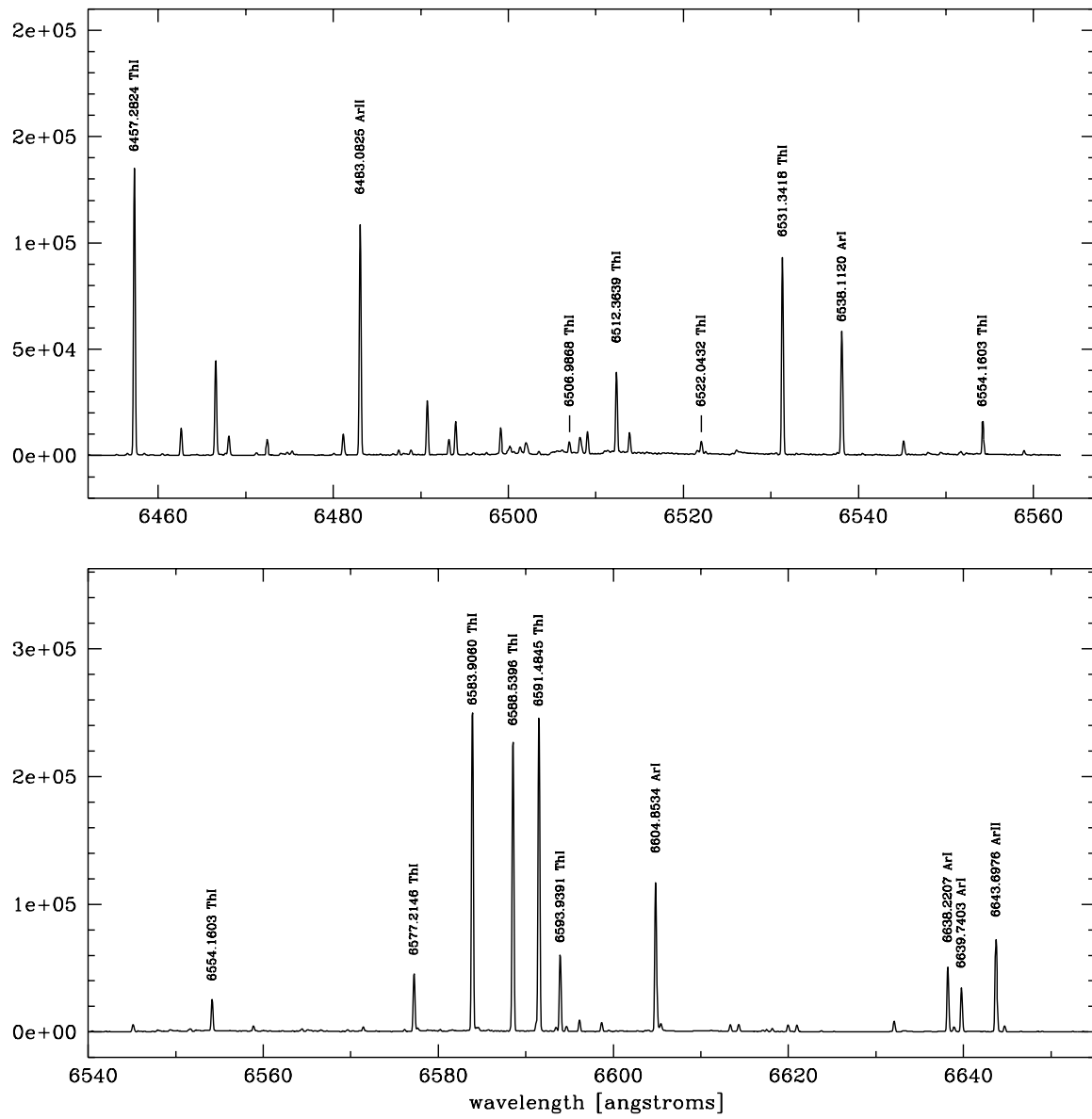


Figure 6.3: Th-Ar spectrum around  $\lambda 5860 \text{ \AA}$  ( $NaD$  lines).



**Figure 6.4:** Th-Ar spectrum in the wavelength range  $\lambda 6460 - 6640 \text{ \AA}$  (around  $H\alpha$  line).

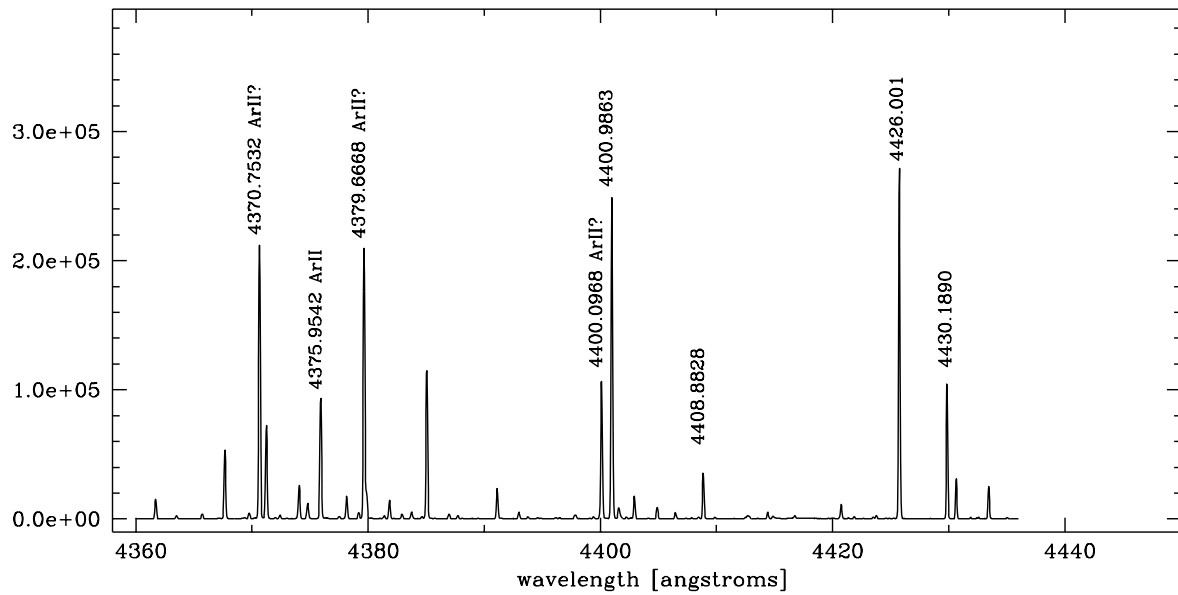


Figure 6.5: Th-Ar spectrum around  $\lambda 4400 \text{ \AA}$ .

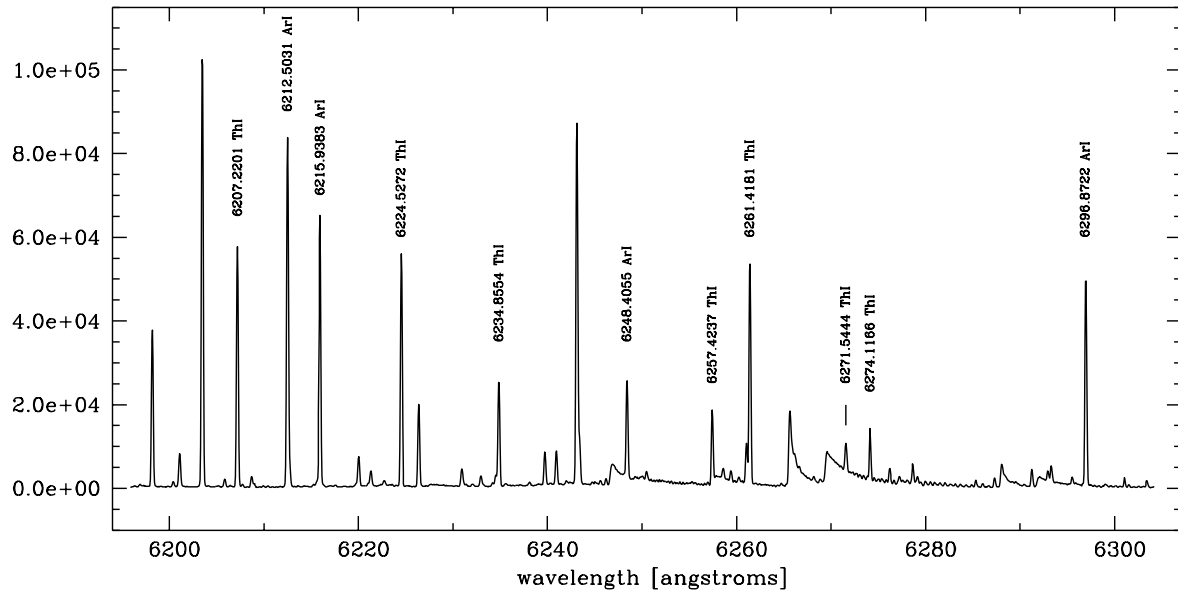


Figure 6.6: Th-Ar spectrum around  $\lambda 6250 \text{ \AA}$ .